

One-dimensional ordering of Ge nanoclusters along atomically straight steps of Si(111)

Takeharu Sekiguchi,^{a)} Shunji Yoshida, and Kohei M. Itoh

Department of Applied Physics and Physico-Informatics, Keio University, 3-14-1, Hiyoshi, Kokohu-ku, Yokohama 223-8522, Japan and Core Research for Evolutional Science and Technology, Japan Science and Technology Agency, Kawaguchi Center Building, 4-1-8 Honcho, Kawaguchi, Saitama 332-0012, Japan

Josef Mysliveček and Bert Voigtländer

Institute of Bio and Nanosystems IBN3, Research Center Jülich and Center of Nanoelectric Systems for Information Technology, 52425 Jülich, Germany

(Received 21 July 2006; accepted 28 November 2006; published online 3 January 2007)

Ge nanostructures grown by molecular beam epitaxy on a vicinal Si(111) surface with atomically well-defined steps are studied by means of scanning tunneling microscopy and spectroscopy. When the substrate temperature during deposition is around 250 °C, Ge nanoclusters of diameters less than 2.0 nm form a one-dimensional array of the periodicity 2.7 nm along each step. This self-organization is due to preferential nucleation of Ge on the unfaulted 7×7 half-unit cells at the upper step edges. Scanning tunneling spectroscopy reveals localized electronic states of the nanoclusters. © 2007 American Institute of Physics. [DOI: 10.1063/1.2426890]

Germanium (Ge) forms quantum dots (QDs) on silicon (Si) surfaces in the Stranski-Krastanov (SK) mode.¹⁻³ In order to obtain highly ordered quantum dots of a uniform size on the order of 10 nm towards application of their quantum confinement effect to optoelectronic devices,^{4,5} many techniques have been used,^{3,6} including vertical stacking with spacer Si layers,⁷ control of Ge composition in the QD and/or the substrate,⁸ and prepatterning⁹ or chemical modification^{10,11} of the substrate. In parallel, formation of an ordered array of quantum dots or quantum wires directly on a substrate without the wetting layer has been investigated as an attracting alternative to the SK growth.^{12,13} Such a direct formation can enhance the quantum confinement effect.^{14,15}

On the other hand, self-assembly of one-dimensional (1D) nanostructures such as of Au and CaF₂ has been demonstrated^{16,17} by using regular step arrays on vicinal Si(111) surfaces.¹⁸⁻²⁰ In this letter, we study self-assembly of Ge on such highly ordered step substrate of Si(111)- 7×7 . Scanning tunneling microscopy (STM) reveals the growth mechanism of 1D arrays of Ge nanoclusters along the step edges. Scanning tunneling spectroscopy (STS) on the Ge nanoclusters shows localized electronic states and a semiconducting gap.

We deposited Ge on a vicinal Si(111) surface with atomically well-defined step edges. The surface was prepared in the same manner as described in Ref. 21. We polished small pieces ($0.65 \times 3 \times 13$ mm³) of a nominal (111) Si wafer so as to make 1° miscut (θ_m) toward a $[\bar{1}\bar{1}2]$ direction with an intentional azimuthal misorientation ($\phi_m = 4^\circ$) to orient all the kinks of the steps in the same direction. The samples were introduced into an ultrahigh vacuum chamber and cleaned with flash heating up to 1300 °C followed by quenching to lower than 830 °C within 3 s. Afterwards, the samples were annealed at 800–830 °C for about 10 h with dc current parallel to the steps specifically in the “kink-up” direction (ascending kinks) to extend atomically straight step

edges.²¹ After slowly cooling down to room temperature and confirming the formation of the straight step edges by *in situ* STM, we deposited Ge atoms from a boron nitride crucible in an effusion cell or from an e-beam evaporator. The Ge deposition rate (R) is calibrated by STM measurements of the effective coverage of Ge islands on terraces wider than 500 nm on a nominal Si(111) substrate. The rates R used in this study were 0.011–0.0032 BL/min with the effusion cell and 0.05 BL/min with the e-beam evaporator, where 1 BL corresponds to the complete pseudomorphic biatomic layer of Ge on Si(111). During the deposition, the substrate was kept at a temperature T_s by passing a constant dc current in the kink-up direction. All the STM images and the STS spectra were measured at room temperature. STS spectra are the average of $(dI/dV)/(I/V)$ measured over several equivalent locations on the same sample, using the technique of continuously varying tip-sample separation^{22,23} to enhance the sensitivity near the zero bias voltage.

Figure 1 shows a STM image of the highly ordered Si(111) substrate measured after Ge deposition at $T_s = 250$ °C ($R = 0.011$ BL/min). The deposited amount of Ge, Θ , is 0.13 BL, which is equivalent to the (7×7) half-unit-cell width (2.7 nm) of 1 BL high island along every step on the 1° miscut substrate. We observe that *nanoclusters* of Ge are self-aligned along the *upper* edges of the steps. These nanoclusters are located preferentially within the unfaulted halves of the 7×7 structure right at the upper step edges so that they have lateral sizes less than 2.0 nm and a periodicity of 2.7 nm along the steps.

STM images at lower bias voltages reveal the detailed structure of the step edge beneath the nanoclusters. The Ge nanoclusters appear as protrusions in the STM image at the sample bias voltage of $V_s = +2.0$ V in Fig. 2(a). However, their apparent height decreases with decreasing V_s , and eventually they appear as depressions at $V_s = +0.5$ V, as shown in Fig. 2(b). With $V_s = +0.5$ V, a *nanowire* of 0.67 nm width along the original Si(111) step edge beneath the nanoclusters becomes clearly visible. This nanowire is a decoration of the

^{a)}Electronic mail: sekiguti@appi.keio.ac.jp

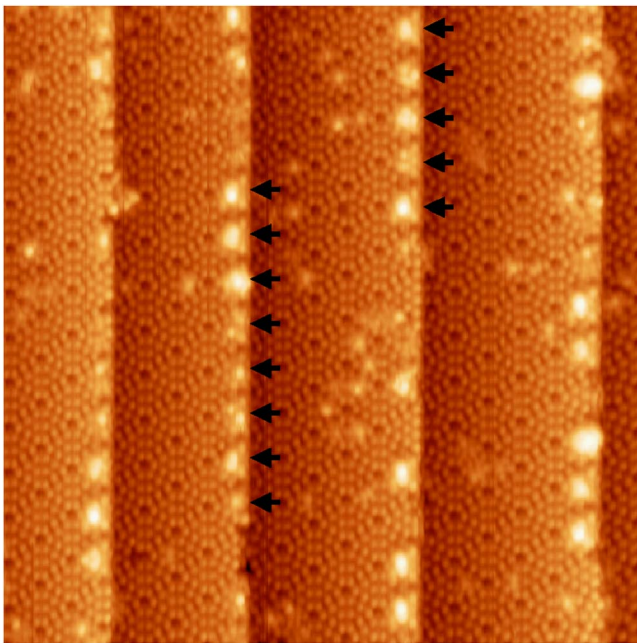


FIG. 1. (Color online) STM image of the vicinal Si(111) template covered with 0.13 BL of Ge deposited at $T_s=250$ °C followed by annealing at the same temperature for 24 min ($\theta_m=1.0^\circ$, $\phi_m=4^\circ$, $R=0.011$ BL/min, and $V_s=+2.0$ V). The step edges before the deposition had the $U(2,0)$ configuration and were terminated at the dimers of the 7×7 structure (Ref. 21). Ge nanoclusters, some of which are indicated by arrows, are aligned along the upper edges of the steps. On the terraces fewer smaller protrusions are seen. The whole area is 46.1×38.1 nm².

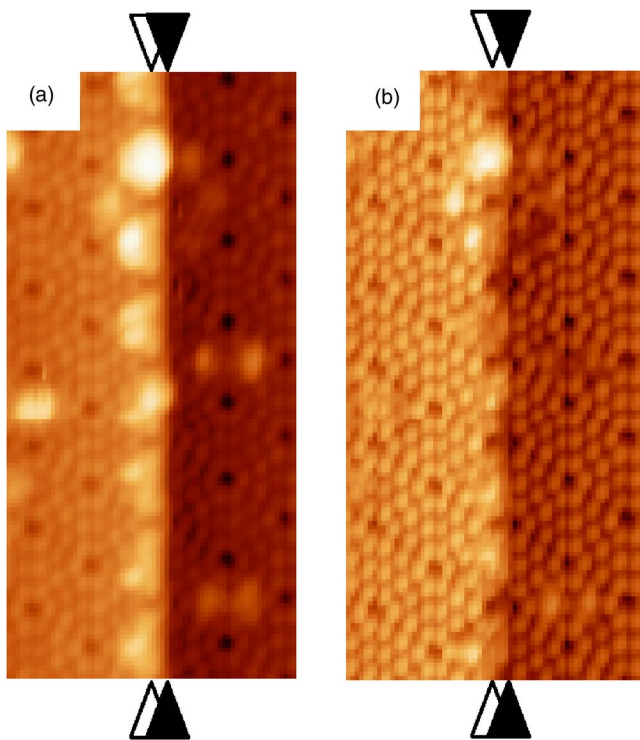


FIG. 2. (Color online) Magnified STM images of the Ge nanoclusters at the upper step edges, clarifying the underlying step structure. Bias voltages are (a) $V_s=+2.0$ V and (b) $+0.5$ V. The growth conditions are the same as used for Fig. 1 apart from the deposition rate ($R=0.0032$ BL/min) and the post-deposition annealing duration (24 min). Open and solid triangles indicate the step position before and after the growth, respectively, and delimit the 0.67 nm wide nanowire that forms on the surface prior to the nucleation of the Ge nanoclusters. Both image areas are 11.7×20.1 nm².

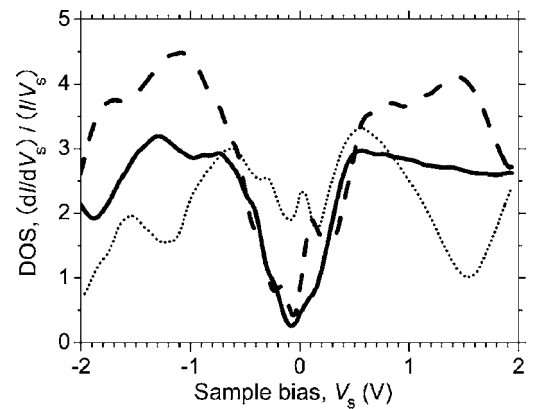


FIG. 3. Room temperature STS spectra of the Ge nanoclusters at the upper step edge (solid line) and on the terraces (dashed line) along with a spectrum of the clean 7×7 structure on the same terrace (dotted line). The growth condition of Ge is as follows: $T_s=250$ °C, $\Theta=0.13$ BL, and $R=0.05$ BL/min.

original Si(111) step edge by Ge atoms and initiates the nanocluster formation at the step edge, similar to the case of Si nanocluster formation on the same substrate.²⁴ Ge nanocluster formation is also observed on the terraces as reported before for the Ge growth on the nominal Si(111) surfaces.^{25–33} It is interesting to note that nucleation of the Ge nanoclusters at the edges occurs predominantly on the unfaulted halves of the 7×7 structure, while nucleation on the terraces occurs preferentially on the faulted halves.^{26,27,31}

We find that, for the particular miscut of our samples (the average terrace width of 18 nm), the substrate temperature $T_s=250$ °C during Ge growth leads to the optimum ordering of the Ge clusters along the step edges. The thermal energy is high enough for Ge atoms to reach the steps leading to the nanocluster formation. At higher $T_s=300$ °C, we observe essentially the same growth mode but the number of the nanoclusters along the upper step edges decreases. This is most likely because the accumulation of Ge atoms is enhanced in the so-called *kink-bunching* regions²¹ due to electromigration along the steps induced by the kink-up dc heating.²⁴ At $T_s=400$ °C, the lower step edges are still initially decorated by the nanowires of the 0.67 nm width like during the 250 °C growth, but the nanocluster formation no longer follows. Instead, a bilayer formation proceeds along the nanowires in a step-flow mode although the resulting 7×7 structure formed by the growth is heavily defective. The thermal energy is high enough for the step flow but not enough to completely rebuild the 7×7 structure.³⁴ The step-flow growth with nearly perfect 7×7 structure may onset at a higher temperature.

Figure 3 shows STS spectra of the Ge nanoclusters at the step edges (solid line) and on the terraces (dashed line) along with a spectrum of the clean terrace without Ge as a reference (dotted line). The spectrum of the clean terrace shows a significant density of states (DOS) at $V_s\approx 0$ V (the Fermi level) and two broad maxima at $V_s\approx -0.6$ V and $V_s\approx +0.5$ V, all of which are well-known features of the STS spectrum of the Si(111)- 7×7 surface at room temperature.²³ Regardless of the position, along the step edges or on the terraces, the spectra of the Ge nanoclusters are very similar and distinctly different from that of the Si surface. Compared to the clean surface DOS, the DOS of the Ge clusters is significantly lowered around the Fermi level between $V_s\approx$

−0.3 V and $V_s \approx +0.2$ V. This lowering is caused by Ge atoms that saturate the adatom dangling bond states of the Si(111)- 7×7 surface that are otherwise the dominating contribution to the surface DOS at the Fermi level.²³ On the other hand, the DOS of the Ge clusters is increased at $V_s \approx -1.3$ V and $V_s \approx +1.5$ V. This indicates that the Ge nanoclusters have localized electronic states. From the size and shape of the Ge nanoclusters we can conclude that they contain <10 atoms.²⁵ Thus, the clusters do not develop bulk band electronic structure and we cannot ascribe the localized states to the quantum confinement of free charge carriers inside the nanocluster.³⁵ Rather, we assign the localized states to the modified surface DOS in the presence of the Ge atoms.

A question remains regarding the composition of the Ge nanoclusters. A recent STM study showed that a Ge atom adsorbed on the 7×7 structure of the Si(111) surface can substitute a Si atom at the topmost adatom site to form the Ge adatom state S_4 .³⁶ This suggests the possibility that Si atoms substituted by Ge on the terrace can migrate to the step edges and be incorporated into the Ge clusters formed along the edges, so that a partial Ge–Si intermixing in the clusters is possible.

In conclusion, we have established an experimental procedure to prepare self-organized 1D arrays of 2-nm-wide Ge clusters along the atomically straight step edges on the vicinal Si(111) substrate. The STS spectra of the nanoclusters show localized electronic states with a semiconducting gap.

The authors would like to acknowledge V. Cherepanov and K. Romanyuk for the expert assistance with the STS measurements. This work is supported in part by a Grant-in-Aid for Scientific Research in a Priority Area “Semiconductor Nanospintronics” Grant No. 14076215.

¹D. J. Eaglesham and M. Cerullo, Phys. Rev. Lett. **64**, 1943 (1990).

²N. Motta, J. Phys.: Condens. Matter **14**, 8353 (2002).

³J. Stangl, V. Holý, and G. Bauer, Rev. Mod. Phys. **76**, 725 (2004).

⁴G. Abstreiter, P. Schittenhelm, C. Engel, E. Silveira, A. Zrenner, D. Meertens, and W. Jäger, Semicond. Sci. Technol. **11**, 1521 (1996).

⁵J. Drucker, IEEE J. Quantum Electron. **38**, 975 (2002).

⁶K. Brunner, Rep. Prog. Phys. **65**, 27 (2002).

⁷J. Tersoff, C. Teichert, and M. G. Lagally, Phys. Rev. Lett. **76**, 1675 (1996).

⁸A. Ronda and I. Berbezier, Physica E (Amsterdam) **23**, 370 (2004).

⁹A. Sgarlata, P. D. Szkutnik, A. Balzarotti, N. Motta, and F. Rosei, Appl. Phys. Lett. **83**, 4002 (2003).

¹⁰O. G. Schmidt, C. Lange, K. Eberl, O. Kienzle, and F. Ernst, Appl. Phys. Lett. **71**, 2340 (1997).

¹¹A. A. Shklyarev, M. Shibata, and M. Ichikawa, Phys. Rev. B **62**, 1540 (2000).

¹²K. Yoo, A.-P. Li, Z. Zhang, H. H. Weitering, F. Flack, M. G. Lagally, and J. F. Wendelken, Surf. Sci. **546**, L803 (2003).

¹³H. Sunamura, N. Usami, Y. Shiraki, and S. Fukatsu, Appl. Phys. Lett. **68**, 1847 (1996).

¹⁴J. Wan, G. L. Jin, Z. M. Jiang, Y. H. Luo, J. L. Liu, and K. L. Wang, Appl. Phys. Lett. **78**, 1763 (2001).

¹⁵A. P. Li, F. Flack, M. G. Lagally, M. F. Chisholm, K. Yoo, Z. Zhang, H. H. Weitering, and J. F. Wendelken, Phys. Rev. B **69**, 245310 (2004).

¹⁶F. J. Himpsel, A. Kirakosian, J. N. Crain, J.-L. Lin, and D. Y. Petrovykh, Solid State Commun. **117**, 149 (2001).

¹⁷F. J. Himpsel, J. L. McChesney, J. N. Crain, A. Kirakosian, V. Pérez-Dieste, N. L. Abbott, Y.-Y. Luk, P. F. Nealey, and D. Y. Petrovykh, J. Phys. Chem. B **108**, 14484 (2004).

¹⁸J. Viernow, J.-L. Lin, D. Y. Petrovykh, F. M. Leibsle, F. K. Men, and F. J. Himpsel, Appl. Phys. Lett. **72**, 948 (1998).

¹⁹J.-L. Lin, D. Y. Petrovykh, J. Viernow, F. K. Men, D. J. Seo, and F. J. Himpsel, J. Appl. Phys. **84**, 255 (1998).

²⁰A. Kirakosian, R. Bennowitz, J. N. Crain, Th. Fauster, J.-L. Lin, D. Y. Petrovykh, and F. J. Himpsel, Appl. Phys. Lett. **79**, 1608 (2001).

²¹S. Yoshida, T. Sekiguchi, and K. M. Itoh, Appl. Phys. Lett. **87**, 031903 (2005).

²²J. A. Stroscio and R. M. Feenstra, in *Scanning Tunneling Microscopy, Methods of Experimental Physics*, edited by J. A. Stroscio and W. J. Kaiser (Academic, San Diego, 1993), Vol. 27, p. 95.

²³J. Mysliveček, A. Stróžeczka, J. Steffl, P. Sobotík, I. Ošťádal, and B. Voigtländer, Phys. Rev. B **73**, 161302 (2006).

²⁴T. Sekiguchi, S. Yoshida, and K. M. Itoh, Phys. Rev. Lett. **95**, 106101 (2005).

²⁵H. Asaoka, V. Cherepanov, and B. Voigtländer, Surf. Sci. **588**, 19 (2005).

²⁶Y. P. Zhang, L. Yan, S. S. Xie, S. J. Pang, and H.-J. Gao, Surf. Sci. **497**, L60 (2002).

²⁷Y. P. Zhang, L. Yan, S. S. Xie, S. J. Pang, and H.-J. Gao, Appl. Phys. Lett. **79**, 3317 (2001).

²⁸L. Yan, Y. Zhang, H. Gao, S. Xie, and S. Pang, Surf. Sci. **506**, L255 (2002).

²⁹F. Ratto and F. Rosei, Surf. Sci. **530**, 221 (2003).

³⁰Z. A. Ansari, T. Arai, and M. Tomitori, Surf. Sci. **574**, L17 (2005).

³¹Z. A. Ansari, M. Tomitori, and T. Arai, Appl. Phys. Lett. **88**, 171902 (2006).

³²L. Yan, H. Yang, H. Gao, S. Xie, and S. Pang, Surf. Sci. **498**, 83 (2002).

³³E. Vasco, Surf. Sci. **575**, 247 (2005).

³⁴M. Suzuki and Y. Shigeta, Surf. Sci. **539**, 113 (2003).

³⁵T. Maltezopoulos, A. Bolz, C. Meyer, C. Heyn, W. Hansen, M. Morgenstern, and R. Wiesendanger, Phys. Rev. Lett. **91**, 196804 (2003).

³⁶Y. L. Wang, H.-J. Gao, H. M. Guo, S. Wang, and S. T. Pantelides, Phys. Rev. Lett. **94**, 106101 (2005).